GRAN SASSO SCIENCE INSTITUTE
SCHOOL OF ADVANCED STUDIES
Scuola Universitaria Superiore

GSSI Astroparticle Colloquium – 23rd January 2019

The Quest for non-Gaussian Signals from the Early Universe

Sabino Matarrese

- Physics & Astronomy Dept. “G. Galilei”, University of Padova, Italy
- INFN Sezione di Padova
- INAF Osservatorio Astronomico di Padova
- GSSI L’Aquila

Why (non-) Gaussian?

The Gaussian paradigm

Gaussian ⟺ free (i.e. non-interacting) field

large-scale phase coherence ⟺ non-linear gravitational dynamics

How to motivate non-Gaussian initial conditions?

Going beyond the Gaussian hypothesis in Cosmology

Historical outline:

1977 Groth and Peebles compute the 3-pt function of galaxies: direct evidence that the LSS is non-Gaussian. Is this only the effect of non-linear gravitational clustering?

1980 Strongly non-Gaussian initial conditions studied in the eighties.

2001 Determination of bispectrum for PSCz (Feldman et al. 2001) and 2dF galaxies (Verde et al. 2002)

1990 New era with f_{NL} non-Gaussian (NG) models from inflation (Salopek & Bond 1991; Gangui et al. 1994: $f_{NL} \sim 10^{-2}$; Verde et al. 1999; Komatsu & Spergel 2001; Acquaviva et al. 2002; Maldacena 2002; + many models with higher f_{NL}).

2000 Primordial NG (PNG) gradually emerged as a new "smoking gun" of (non-standard) inflation models, which complements the search for primordial gravitational waves (PGW). PNG probes interactions among fields at the highest energy scales.

2013 Is this route still viable, given the very stringent Planck constraints?

The view on Non-Gaussianity … circa 1990

Moscardini, Lucchin, Matarrese & Messina 1991

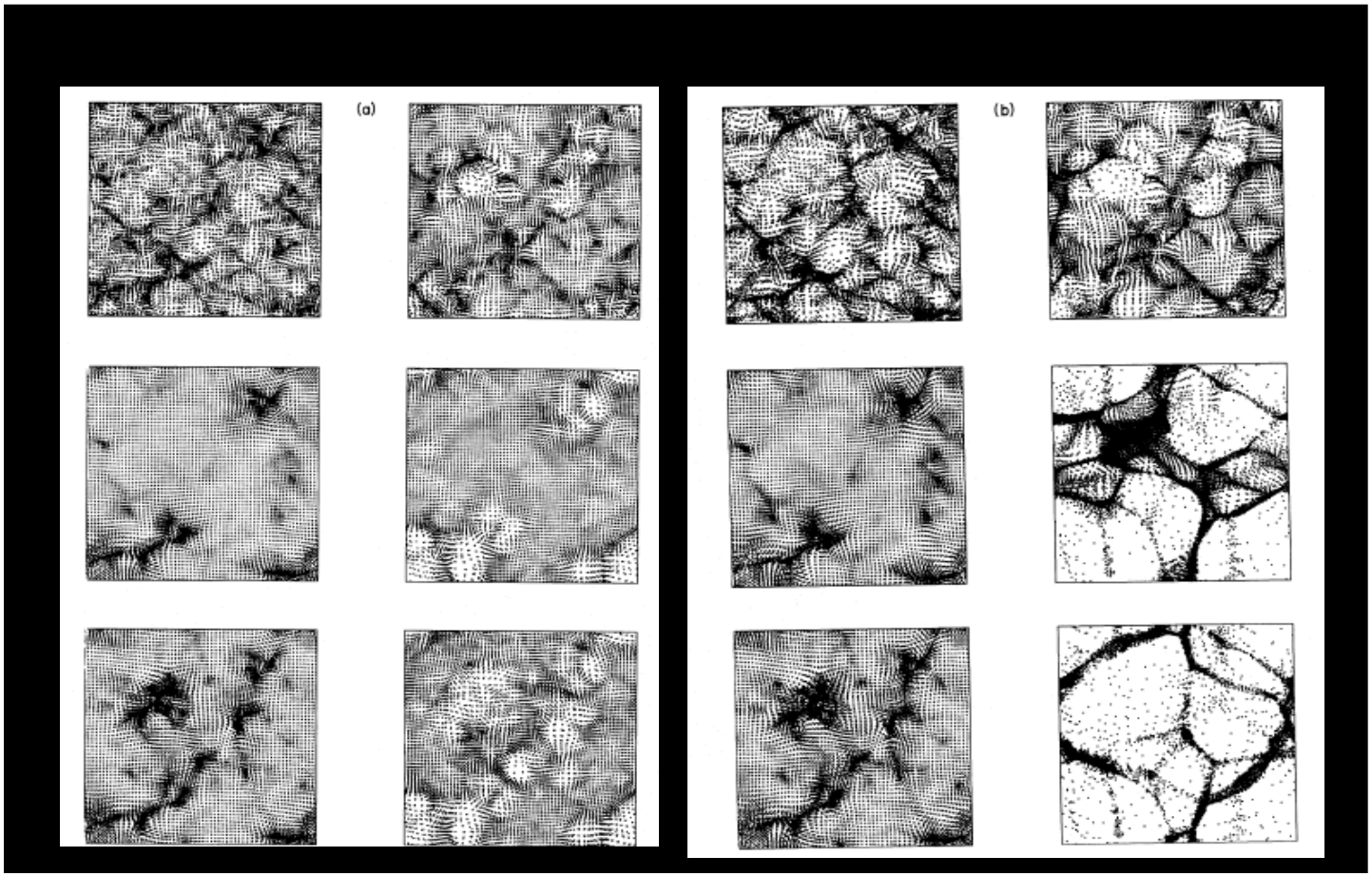

The present view on Primordial non-Gaussianity (PNG) in cosmological perturbations

- ✓ Alternative structure formation models of the late eighties considered strongly non-Gaussian primordial fluctuations.
- ✓ The increased accuracy in CMB and LSS observations has, however, excluded such an extreme possibility.
- ✓ The present-day challenge is to either detect or constrain mild or weak deviations from primordial Gaussian initial conditions.
- ✓ Deviations of this type are not only possible but are generically predicted in the standard perturbation generating mechanism provided by inflation.

Late nineties: simple-minded NG model

Many primordial (inflationary) models of non-Gaussianity can be represented in configuration space by the simple formula (Salopek & Bond 1990; Gangui et al. 1994; Verde et al. 1999; Komatsu & Spergel 2001)

$$\Phi = \phi_L + f_{NL} * (\phi_L^2 - \langle \phi_L^2 \rangle) + g_{NL} * (\phi_L^3 - \langle \phi_L^2 \rangle \phi_L) + \dots$$

where Φ is the large-scale gravitational potential (more precisely $\Phi = 3/5\ \zeta$ on superhorizon scales, where ζ is the gauge-invariant comoving curvature perturbation), ϕ_L its linear Gaussian contribution and f_{NL} the dimensionless *non-linearity parameter* (or more generally *non-linearity function*). The percent of non-Gaussianity in CMB data implied by this model is

NG % ~ 10^{-5} $|f_{NL}|$

~ 10^{-10} $|g_{NL}|$

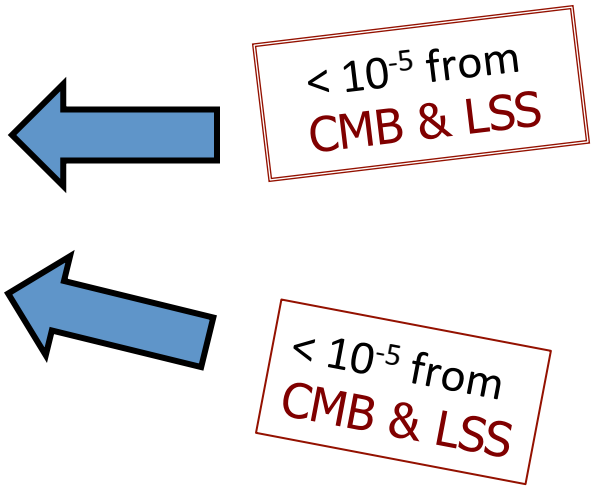

"non-Gaussian = non-dog"
(Ya.B. Zel'dovich)

Non-Gaussianity in the Initial Conditions

Testable predictions of inflation

- Cosmological aspects
  - Critical density Universe
  - Almost scale-invariant and **nearly Gaussian**, adiabatic density fluctuations
  - Almost scale-invariant stochastic background of relic gravitational waves
- Particle physics aspects
  - **Nature of the inflaton**
  - Inflation energy scale

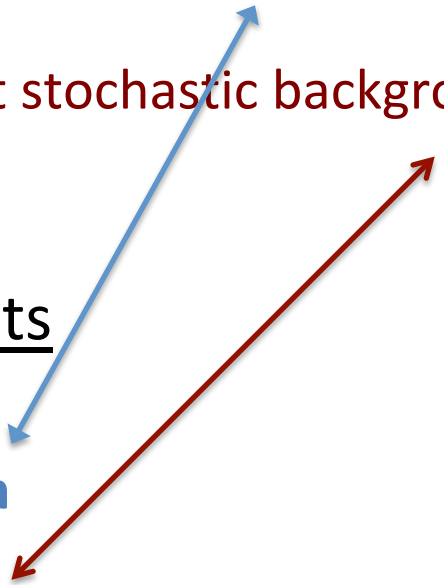

PNG probes physics of the Early Universe

- PNG amplitude and shape measures deviations from standard inflation, perturbation generating processes after inflation, initial state before inflation, ...
- Models yielding the same predictions for scalar spectral index and tensor-to-scalar ratio might be distinguishable in terms of NG features.
- We should aim at "reconstructing" the inflationary action, starting from measurements of a few observables (like n_S, r, n_T, f_{NL}, g_{NL}, etc. …), just like in the nineties we aimed reconstructing of the inflationary potential (see e.g. the revival of the latter industry after the Bicep2 claim of PGW detection, ...).

NG requires going beyond the standard power-spectrum statistics

- The simplest statistics (but not fully general) measuring NG is the 3-point function or its Fourier transform, the "bispectrum":

$$\langle\phi(\mathbf{k}_1)\phi(\mathbf{k}_2)\phi(\mathbf{k}_3)\rangle = (2\pi)^3\delta^{(3)}(\mathbf{k}_1+\mathbf{k}_2+\mathbf{k}_3)\, B_\phi(k_1,k_2,k_3)$$

which carries shape information.

- In our simple linear + quadratic model above, the bispectrum of the gravitational potential reads:

$$B_\phi(k_1,k_2,k_3) = 2f_{NL}\,[P_\phi(k_1)P_\phi(k_2) + \text{cyclic terms}]$$

(by direct application of Wick's theorem), where

$$\langle\phi(\mathbf{k}_1)\phi(\mathbf{k}_2)\rangle = (2\pi)^3\delta^{(3)}(\mathbf{k}_1+\mathbf{k}_2)\, P_\phi(k_1)$$

Where does NG come from (in standard inflation)?

- *Falk et al. (1993)* found $f_{NL} \sim \xi \sim \varepsilon^2$ (from non-linearity in the inflaton potential in a fixed de Sitter space) in the standard single-field slow-roll scenario

- *Gangui et al. (1994)*, using stochastic inflation found $f_{NL} \sim \varepsilon, \eta$ (from second-order gravitational corrections during inflation). *Acquaviva et al. (2003)* and *Maldacena (2003)* confirmed this estimate (up to numerical factors and momentum-dependent terms) with a full second-order approach. Weinberg extended the calculation of the bispectrum to 1-loop. One of these terms gives rise to the so-called "consistency relation", according to which found $f_{NL} = - 5/12(n_s-1)$ It has been shown that this term can be gauged away by a non-linear rescaling of coordinates, up to sub-leading terms. The only residual term is proportional to ε i.e. to the amplitude of tensor modes. See however comments on this point, later on.

Bispectrum & PNG: theoretical expectations

- Primordial NG probed fundamental physics during inflation, being sensitive to ***(self-)interactions*** of fields present during inflation (different inflationary models predict different ***amplitudes and shapes*** of the bispectrum)

- Standard models of slow-roll inflation predict only a ***tiny deviation from Gaussianity*** (Salopek & Bond ‘90; Gangui, Lucchin, Matarrese & Mollerach 1995; Acquaviva, Bartolo, Matarrese & Riotto 2003; Maldacena 2003), arising from ***non-linear gravitational interactions*** during inflation.

- Searching for deviations from this *standard paradigm* is interesting *per-se,* for theoretically well-motivated models of inflation and, as shown in *Planck results, can* ***severely limit*** various classes of inflationary models beyond the simplest paradigm. PNG probes interactions among particles at inflation energy scales. See literature on probing string-theory via oscillatory PNG (Arkani-Hamed & Maldacena 2015 “Cosmological collider physics”; Silverstein 2017 “*The dangerous irrelevance of string theory*”).

Evaluating NG: from inflation to the present universe

Evaluate non-Gaussianity during inflation by a self-consistent second-order calculation (or equivalent techniques, …).

Evolve scalar (vector) and tensor perturbations to second order after inflation outside the horizon, matching conserved second-order gauge-invariant variable, such as the comoving curvature perturbation $\zeta^{(2)}$ (or non-linear generalizations of it), to its value at the end of inflation (accurately accounting for reheating).

Evolve them consistently after they re-enter the Hubble radius → i.e. compute second-order radiation transfer function for CMB and second-order matter transfer function for LSS (few codes already available!)

Starting point: the curvature (gravitational potential) bispectrum

Bispectrum of primordial curvature perturbations

Amplitude

Shape

$$\langle \Phi(\vec{k}_1)\Phi(\vec{k}_2)\Phi(\vec{k}_3)\rangle = (2\pi)^3\delta^{(3)}(\vec{k}_1+\vec{k}_2+\vec{k}_3) f_{\rm NL} F(k_1,k_2,k_3)$$

NOTE: The tree-level contribution to the bispectrum comes from **second-order perturbation theory**, just like linear perturbation theory yields the tree-level contribution to the power-spectrum. Hence one needs to afford GR second-order perturbation theory during and after inflation, which also requires proper handling of vector and tensor modes.

there are more shapes of non-Gaussianity from inflation than ... stars in the sky

Models behind bispectrum shapes (... a few of them)

- **local** shape: Multi-field models, Curvaton, Ekpyrotic/cyclic, etc. ...
- **equilateral** shape: Non-canonical kinetic term, DBI, K-inflation, Higher-derivative terms, Ghost, EFT approach
- **orthogonal** shape: Distinguishes between variants of non-canonical kinetic term, higher-derivative interactions, Galilean inflation
- **flattened** shape: non-Bunch-Davies initial state and higher-derivative interactions, models where a Galilean symmetry is imposed. The flat shape can be written in terms of equilateral and orthogonal.

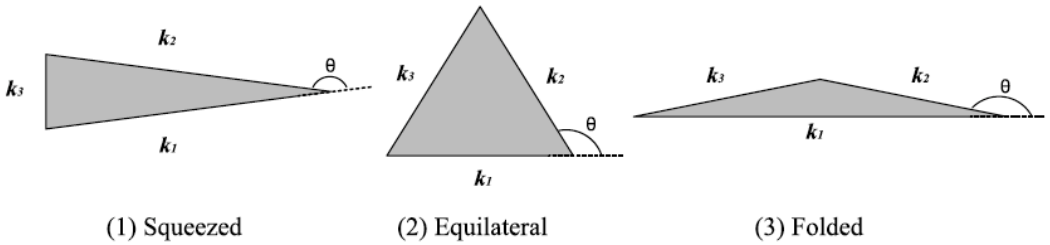

(1) Squeezed (2) Equilateral (3) Folded

NG shapes: local

Bispectrum peaks for squeezed triangles $k_1 \ll k_2 \sim k_3$

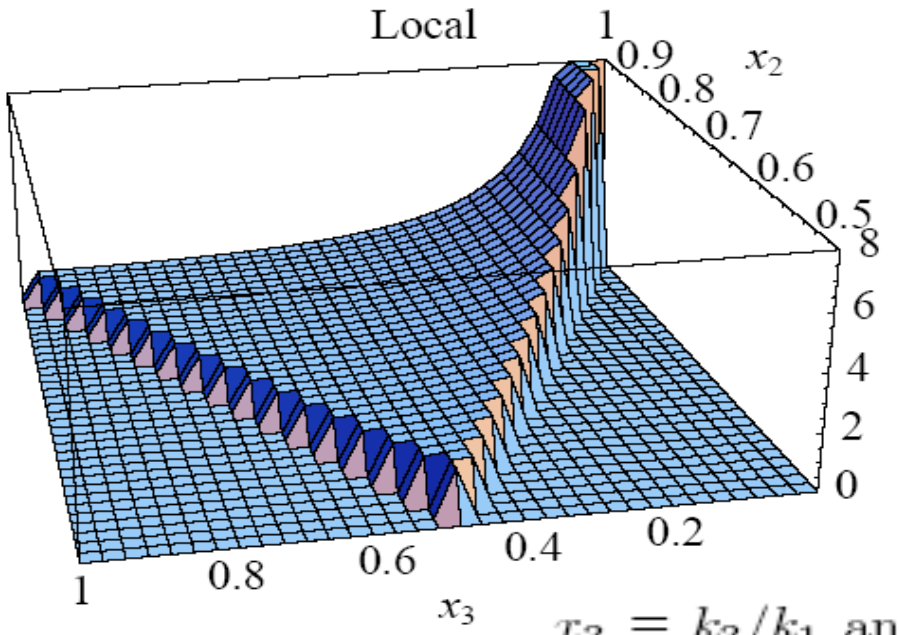

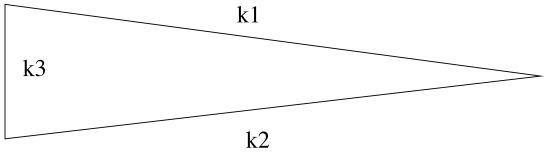

$$F(1,x_2,x_3)x_2^2x_3^2$$

$x_3 \equiv k_3/k_1$ and $x_2 \equiv k_2/k_1$

Babich et al. astro-ph/0405356

$$\Phi(\mathbf{x}) = \Phi_L(\mathbf{x}) + f_{\rm NL}\Phi_L^2(\mathbf{x})$$

Non-linearities develop outside the horizon during or immediately after inflation (e.g. multifield models of inflation)

NG shapes: equilateral

Bispectrum peaks for equilateral triangles: $k_1=k_2=k_3$

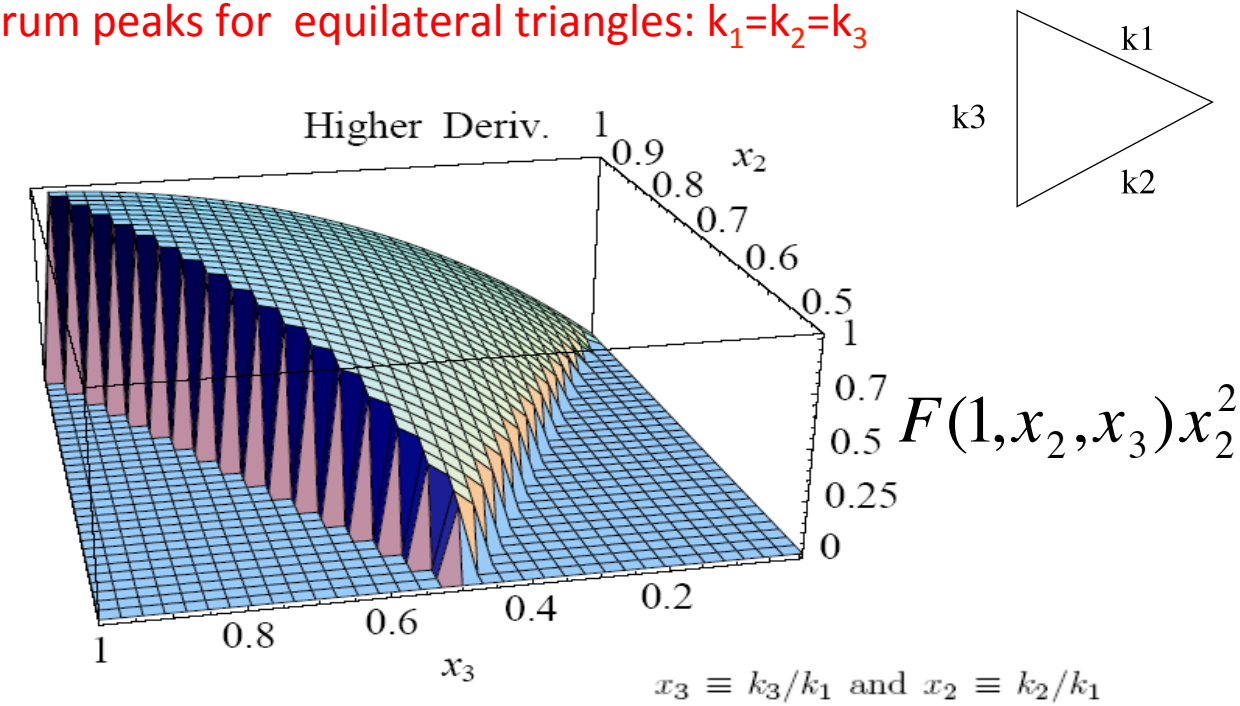

Babich et al. (2004)

Single field models of inflation with non-canonical kinetic term L=P(φ, X) where X=(∂ φ)^2 (DBI or K-inflation) where NG comes from higher derivative interactions of the inflaton field

Example: $\dot{\delta\phi}(\nabla\delta\phi)^2$

NG shapes: flattened

Bispectrum peaks for flattened triangles $k_2 = k_1 + k_3$

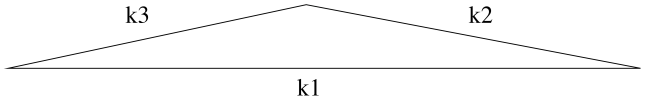

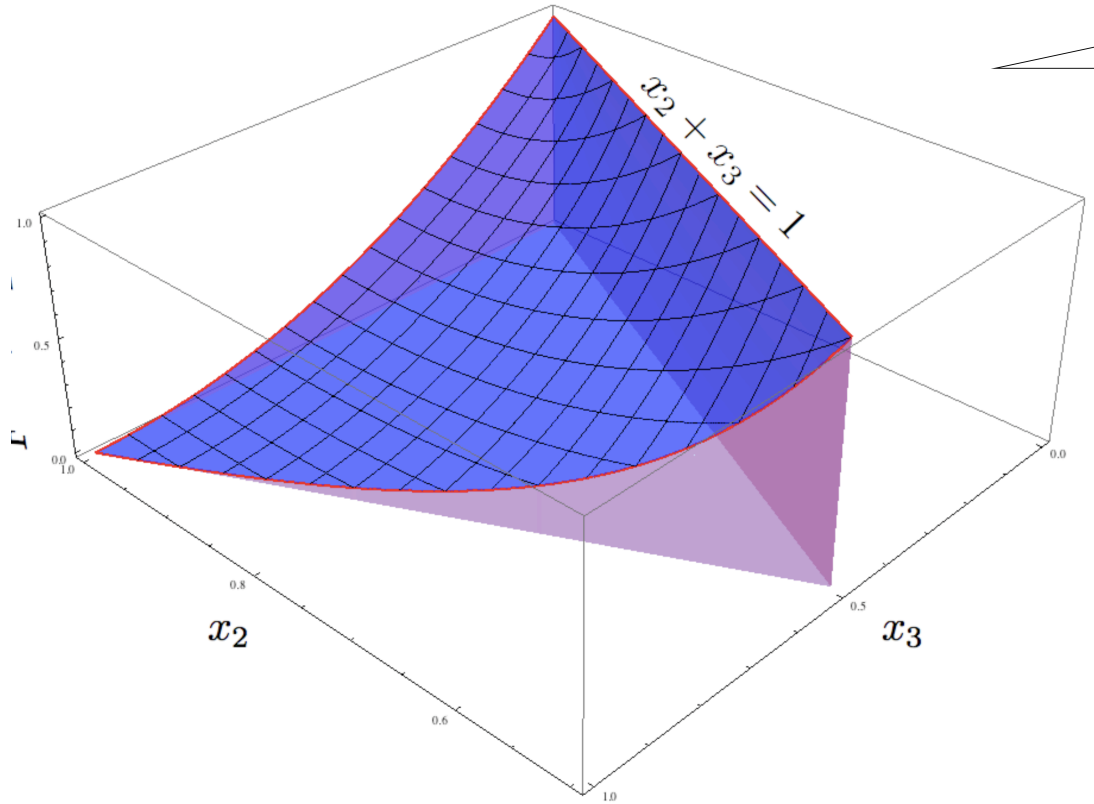

(typical of NG from excited initial states, see Meerburg et al. arXiv:0901.4044; Chen et al. hep-th/0605045; Holman & Tolley arXiv:0710.1302; or from higher derivative interactions, Fasiello, Bartolo, Matarrese, Riotto arXiv:1004.0893)

Non-Gaussianity &
Cosmic Microwave Background (CMB)

The scientific results that we present today are a product of the Planck Collaboration, including individuals from more than 100 scientific institutes in Europe, the USA and Canada

Planck is a project of the European Space Agency, with instruments provided by two scientific Consortia funded by ESA member states (in particular the lead countries: France and Italy) with contributions from NASA (USA), and telescope reflectors provided in a collaboration between ESA and a scientific Consortium led and funded by Denmark.

The *Planck* legacy

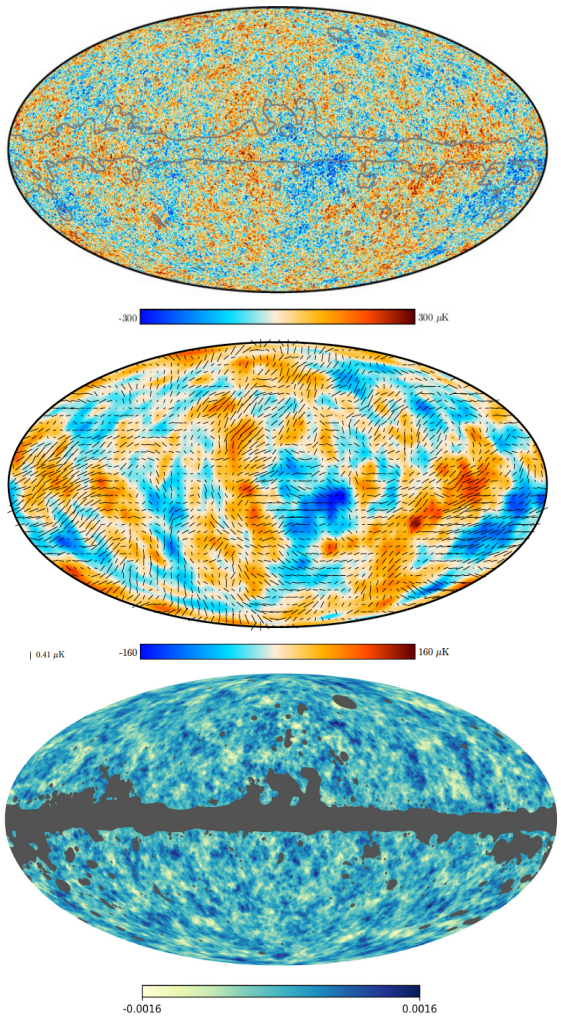

Fig. 6. The *Planck* CMB sky. The top panel shows the 2018, SMICA temperature map. The middle panel shows the polarization field as rods of varying length, superimposed on the temperature map, when both are smoothed at the 5° scale. This smoothing is done for visibility purposes, but the enlarged region presented in Fig. 7 shows that the *Planck* polarization map is dominated by signal at much smaller scales. Both these CMB maps have been masked and inpainted in regions where residuals from foreground emission are expected to be substantial. This mask, mostly around the Galactic plane, is delineated by a grey line in the full resolution temperature map. The bottom panel shows the *Planck* lensing map (derived from $\nabla\phi$, i.e., the E mode of the lensing deflection angle), specifically a minimum variance, Wiener filtered, map obtained from both temperature and polarization information; the unmasked area covers 80.7 % of the sky, which is larger than that used for cosmology.

Planck collaboration 2018 (legacy paper)

The *Planck* legacy

Planck collaboration 2018 (legacy paper)

Table 7. Parameter confidence limits from *Planck* CMB temperature, polarization and lensing power spectra, and with the inclusion of BAO data. The first set of rows gives 68 % limits for the base-ΛCDM model, while the second set gives 68 % constraints on a number of derived parameters (as obtained from the constraints on the parameters used to specify the base-ΛCDM model). The third set below the double line gives 95 % limits for some 1-parameter extensions to the ΛCDM model. More details can be found in Planck Collaboration VI (2018).

Parameter	*Planck* alone	*Planck* + BAO
$\Omega_b h^2$	0.02237 ± 0.00015	0.02242 ± 0.00014
$\Omega_c h^2$	0.1200 ± 0.0012	0.11933 ± 0.00091
$100\theta_{MC}$	1.04092 ± 0.00031	1.04101 ± 0.00029
τ	0.0544 ± 0.0073	0.0561 ± 0.0071
$\ln(10^{10} A_s)$	3.044 ± 0.014	3.047 ± 0.014
n_s	0.9649 ± 0.0042	0.9665 ± 0.0038
H_0	67.36 ± 0.54	67.66 ± 0.42
Ω_Λ	0.6847 ± 0.0073	0.6889 ± 0.0056
Ω_m	0.3153 ± 0.0073	0.3111 ± 0.0056
$\Omega_m h^2$	0.1430 ± 0.0011	0.14240 ± 0.00087
$\Omega_m h^3$	0.09633 ± 0.00030	0.09635 ± 0.00030
σ_8	0.8111 ± 0.0060	0.8102 ± 0.0060
$\sigma_8(\Omega_m/0.3)^{0.5}$	0.832 ± 0.013	0.825 ± 0.011
z_{re}	7.67 ± 0.73	7.82 ± 0.71
Age[Gyr]	13.797 ± 0.023	13.787 ± 0.020
r_*[Mpc]	144.43 ± 0.26	144.57 ± 0.22
$100\theta_*$	1.04110 ± 0.00031	1.04119 ± 0.00029
r_{drag}[Mpc]	147.09 ± 0.26	147.57 ± 0.22
z_{eq}	3402 ± 26	3387 ± 21
k_{eq}[Mpc^{-1}]	0.010384 ± 0.000081	0.010339 ± 0.000063
Ω_K	-0.0096 ± 0.0061	0.0007 ± 0.0019
Σm_ν [eV]	< 0.241	< 0.120
N_{eff}	$2.89^{+0.36}_{-0.38}$	$2.99^{+0.34}_{-0.33}$
$r_{0.002}$	< 0.101	< 0.106

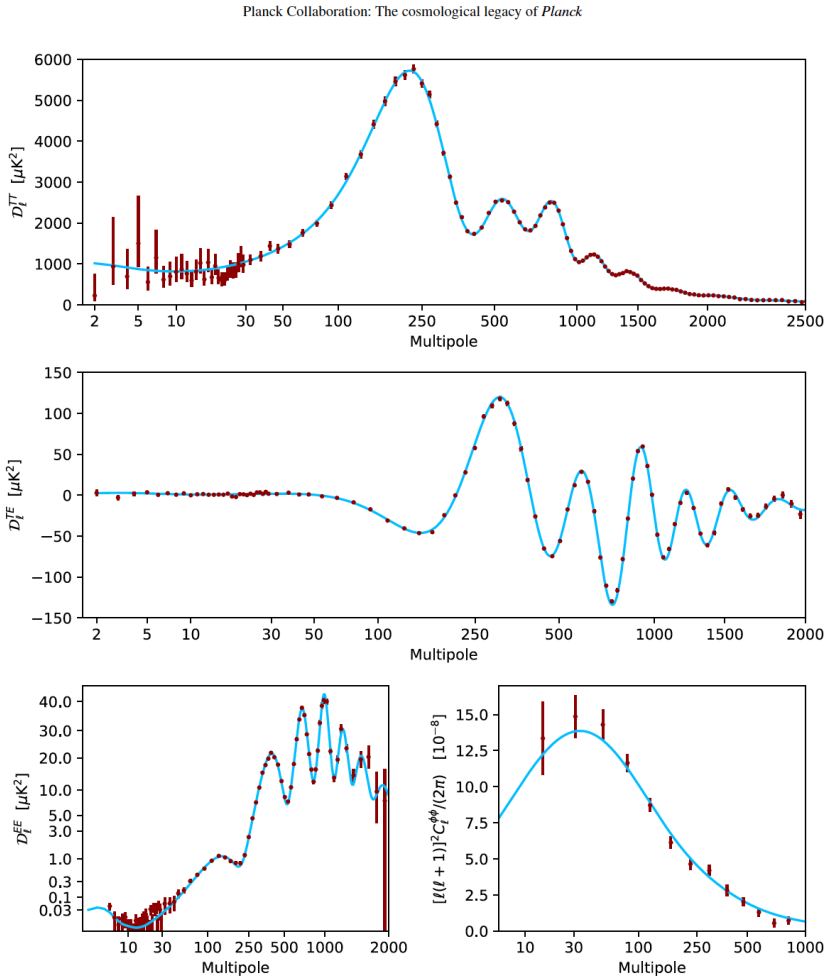

Fig. 9. *Planck* CMB power spectra. These are foreground-subtracted, frequency-averaged, cross-half-mission angular power spectra for temperature (top), the temperature-polarization cross-spectrum (middle), the E mode of polarization (bottom left) and the lensing potential (bottom right). Within ΛCDM these spectra contain the majority of the cosmological information available from *Planck*, and the blue lines show the best-fitting model. The uncertainties of the TT spectrum are dominated by sampling variance, rather than by noise or foreground residuals, at all scales below about $\ell = 1800$ – a scale at which the CMB information is essentially exhausted within the framework of the ΛCDM model. The TE spectrum is about as constraining as the TT one, while the EE spectrum still has a sizeable contribution from noise. The lensing spectrum represents the highest signal-to-noise ratio detection of CMB lensing to date, exceeding 40σ. The anisotropy power spectra use a standard binning scheme (which changes abruptly at $\ell = 30$), but are plotted here with a multipole axis that goes smoothly from logarithmic at low ℓ to linear at high ℓ.

The *Planck* legacy

Planck collaboration
2018 (legacy paper)

Constraints on Inflation Models

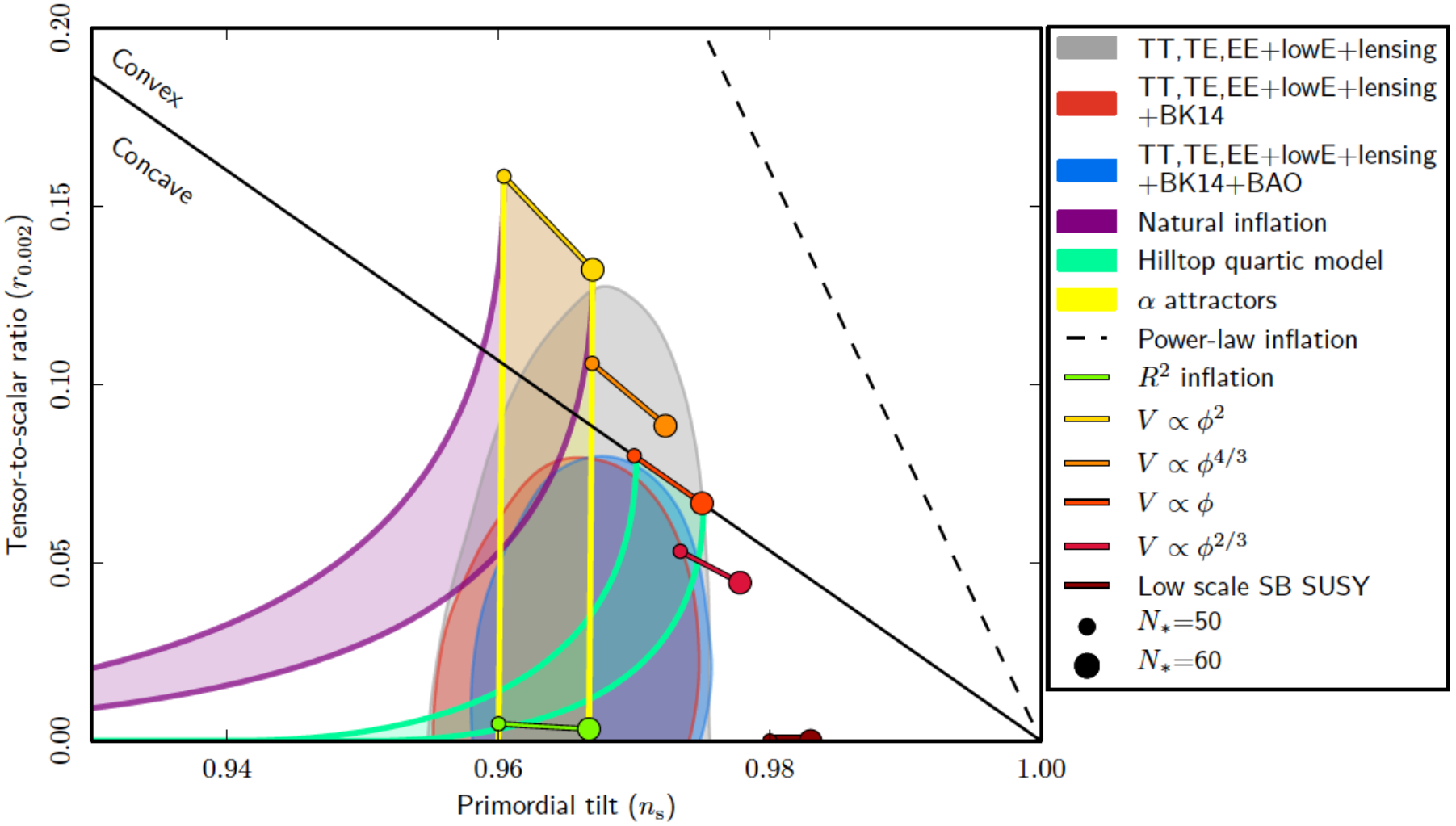

Fig. 23. Limits on the tensor-to-scalar ratio, $r_{0.002}$ as a function of n_S in the ΛCDM model at 95% CL, from *Planck* alone (grey area) or including BICEP2/Keck data 2014 (red) and BAO (blue). Constraints assume negligible running of the inflationary consistency relation and the lines show the predictions of a number of models as a function of the number of e-folds, $N_\star$, till the end of inflation. This can be compared with the middle panel in the top row of Fig. 14 which gives a temporal perspective.

NG CMB simulated maps at *Planck* resolution

temperature

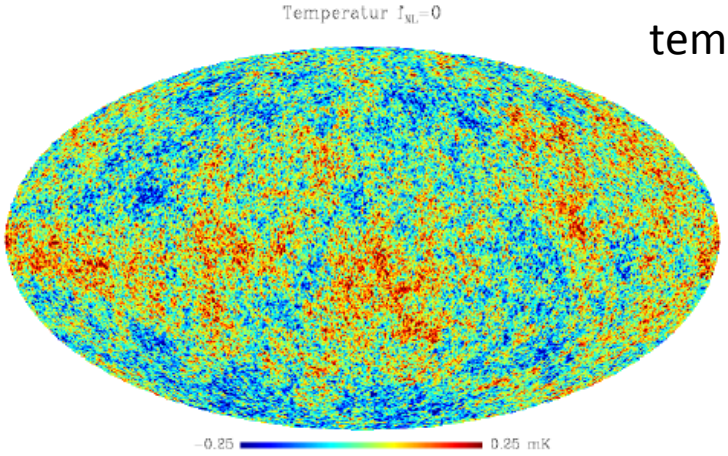

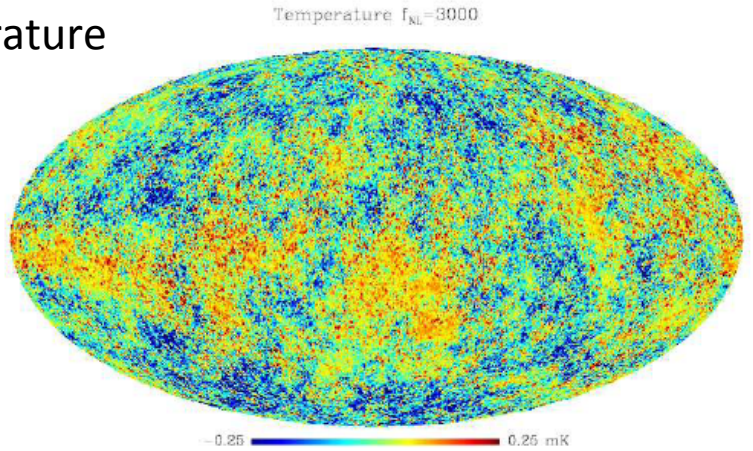

Gaussian

Liguori, Yadav, Hansen, Komatsu, Matarrese & Wandelt 2007

non-Gaussian

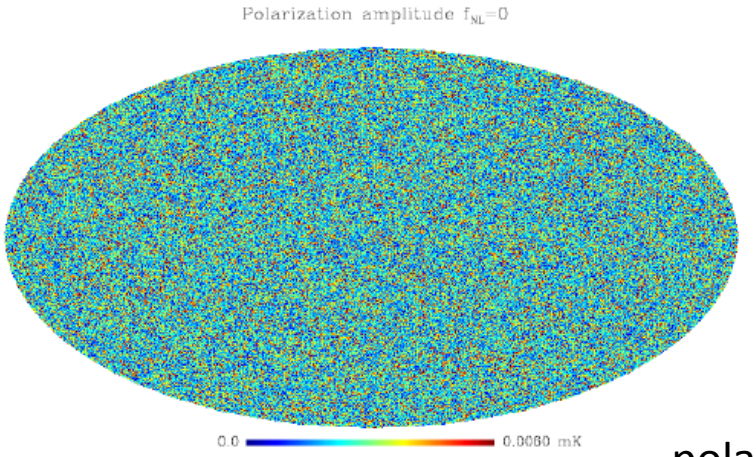

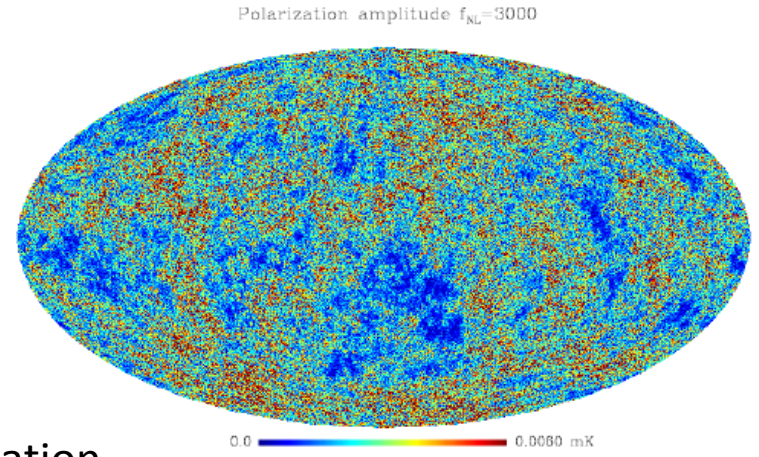

polarization

Planck 2018 results IX: *Planck* collaboration, in preparation (2019)

PNG Planck project (Coordinators: S. Matarrese & B. Wandelt)

- Constrain (with high precision) and/or detect primordial non-Gaussianity (NG) as due to (non-standard) inflation (NG amplitude and shape measure deviations from standard inflation, perturbation generating processes after inflation, initial state before inflation, ...)

- We test: ***local, equilateral, orthogonal*** shapes (+ many more) for the bispectrum and constrain primordial trispectrum parameter g_{NL} (τ_{NL} constrained in previous release).

- We are completing (delivered in a few more weeks) a final, *Planck* legacy release, which will improve the 2015 results in terms of more refined treatment of E-mode polarization (including lower and higher l.

WARNING: this is not a blind search for PNG

- Detecting non-zero primordial bispectrum (e.g. non-zero f_{NL}) proves that the initial seeds were non-Gaussian. Similarly for the trispectrum, etc. …

- But: not detecting non-zero f_{NL} doesn't prove Gaussianity!

- Indeed, there are infinitely many ways PNG can evade observational bounds optimized to search for f_{NL} and similar higher-order parameters.

CMB bispectrum representation

$$B^{m_1 m_2 m_3}_{\ell_1 \ell_2 \ell_3} \equiv \langle a_{\ell_1 m_1} a_{\ell_2 m_2} a_{\ell_3 m_3} \rangle$$

$$= \mathcal{G}^{\ell_1 \ell_2 \ell_3}_{m_1 m_2 m_3} \, b_{\ell_1 \ell_2 \ell_3}$$

Gaunt integrals

$$\mathcal{G}^{\ell_1 \ell_2 \ell_3}_{m_1 m_2 m_3} \equiv \int Y_{\ell_1 m_1}(\hat{\boldsymbol{n}}) \, Y_{\ell_2 m_2}(\hat{\boldsymbol{n}}) \, Y_{\ell_3 m_3}(\hat{\boldsymbol{n}}) \, d^2\hat{\boldsymbol{n}}$$

$$= h_{\ell_1 \ell_2 \ell_3} \begin{pmatrix} \ell_1 & \ell_2 & \ell_3 \\ m_1 & m_2 & m_3 \end{pmatrix},$$

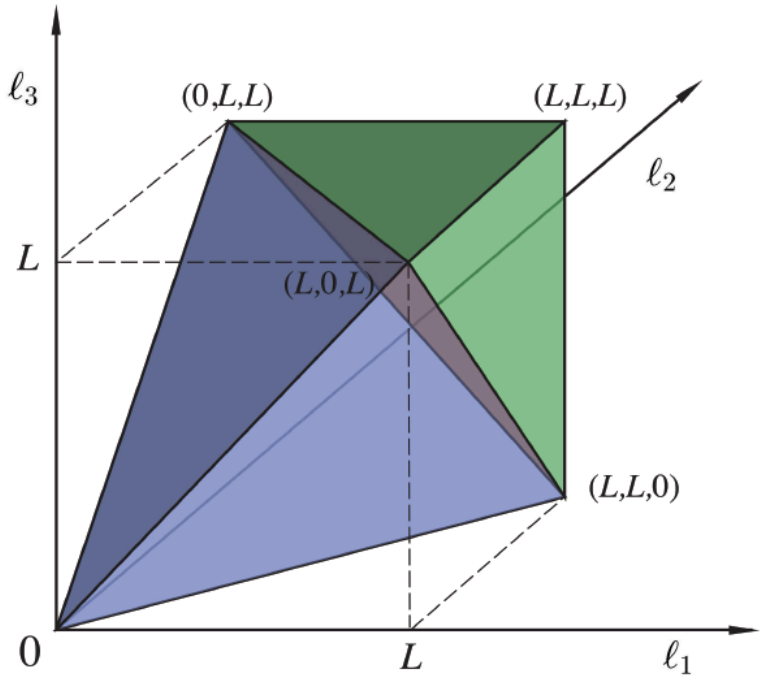

Triangle condition: $\ell_1 \le \ell_2 + \ell_3$ for $\ell_1 \ge \ell_2, \ell_3$, +perms.

Parity condition: $\ell_1 + \ell_2 + \ell_3 = 2n, \quad n \in \mathbb{N},$

Resolution: $\ell_1, \ell_2, \ell_3 \le \ell_{\max}, \quad \ell_1, \ell_2, \ell_3 \in \mathbb{N}.$

Optimal f_{NL} bispectrum estimator

$$\hat{f}_{NL} = \frac{1}{N} \sum B^{m_1 m_2 m_3}_{\ell_1 \ell_2 \ell_3} \left[\left(C^{-1}a\right)^{m_1}_{\ell_1} \left(C^{-1}a\right)^{m_2}_{\ell_2} \left(C^{-1}a\right)^{m_3}_{\ell_3} - 3C^{-1}_{\ell_1 m_1 \ell_2 m_2} \left(C^{-1}a\right)^{m_3}_{\ell_3} \right]$$

The theoretical template needs to be written in separable form. This can be done in different ways and *alternative implementations differ basically in terms of the separation technique adopted and of the projection domain*.

- KSW (Komatsu, Spergel & Wandelt 2003) separable template fitting + Skew-C_l extension (Munshi & Heavens 2010)
- Binned bispectrum (Bucher, Van Tent & Carvalho 2009)
- Modal expansion (Fergusson, Liguori & Shellard 2009)

Bispectrum shapes (modal representation)

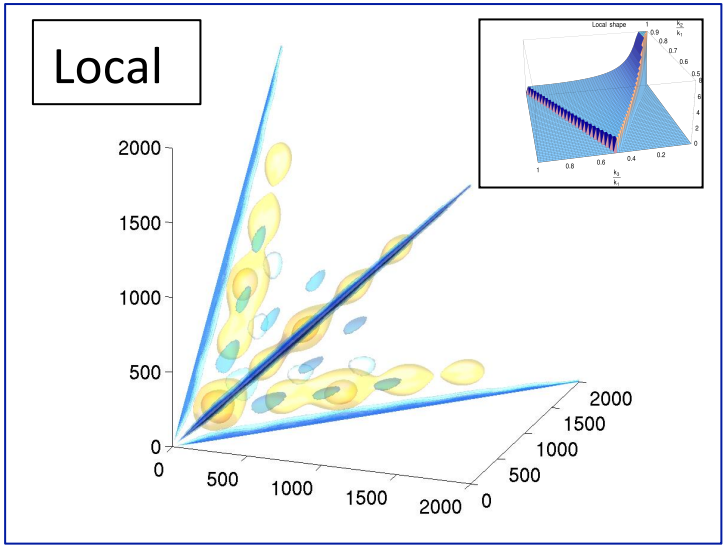

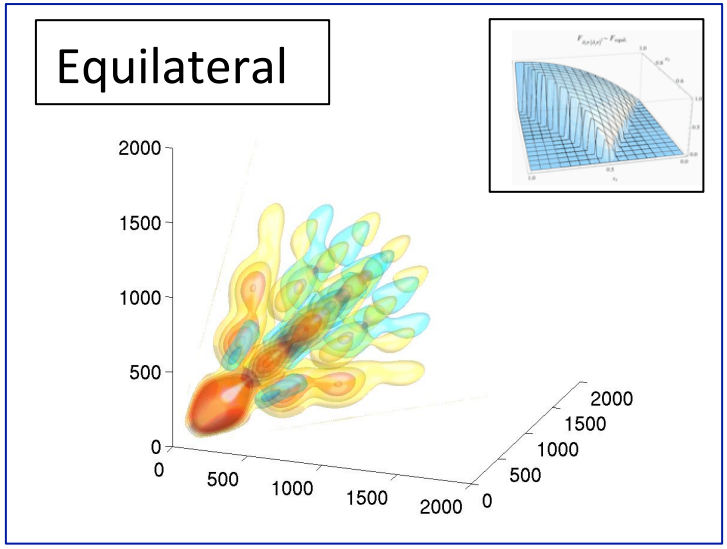

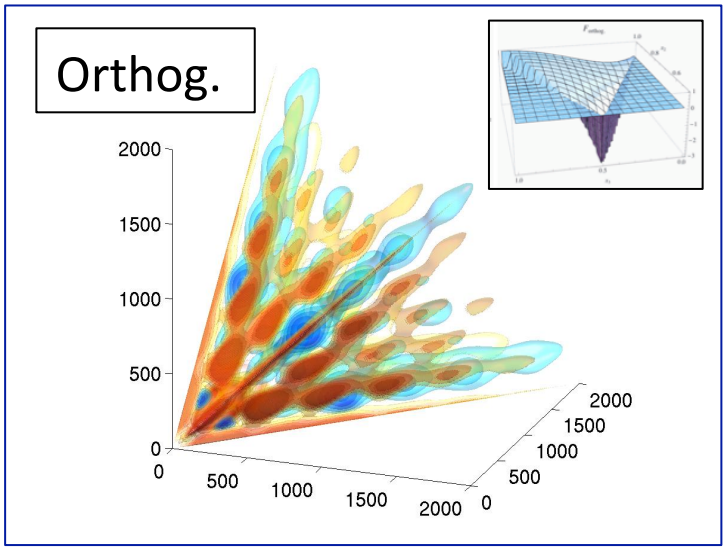

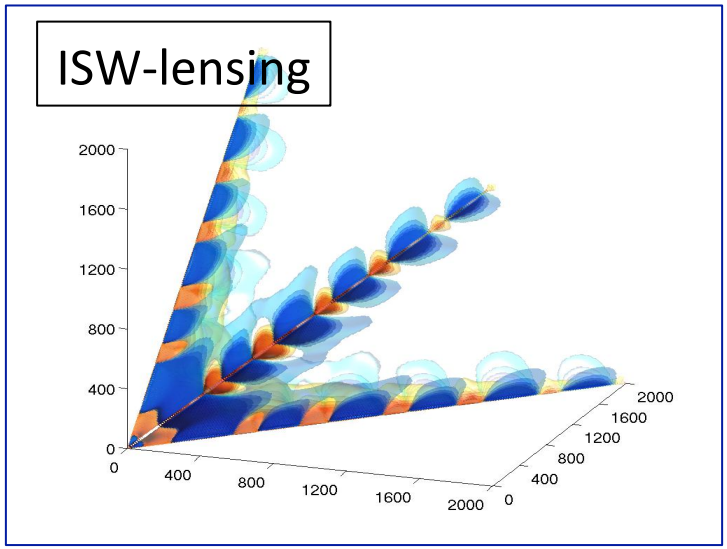

The *Planck* bispectrum (modal; 2015)

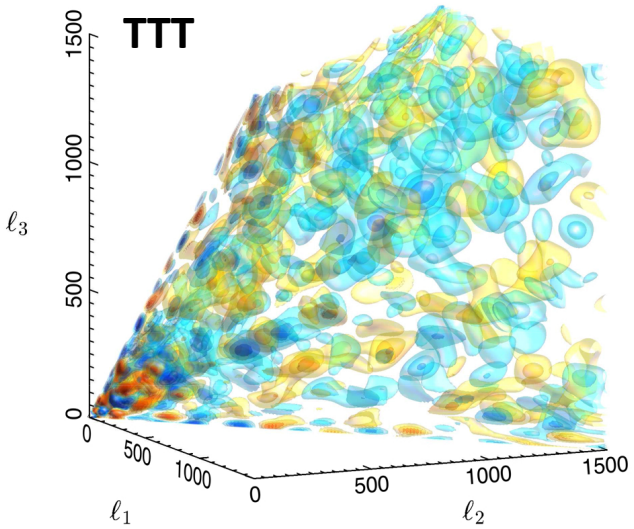

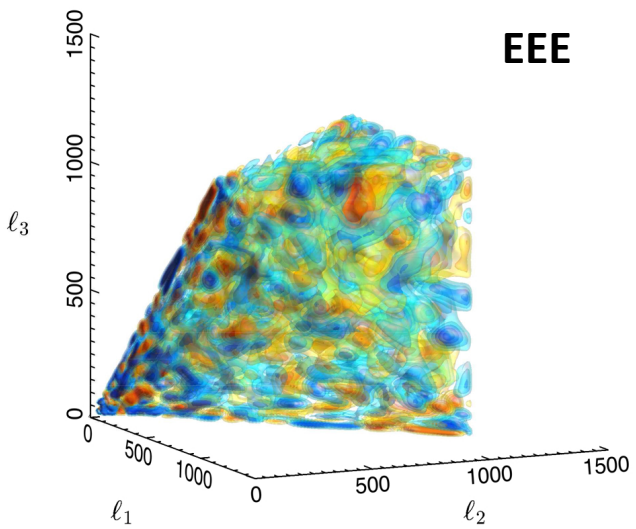

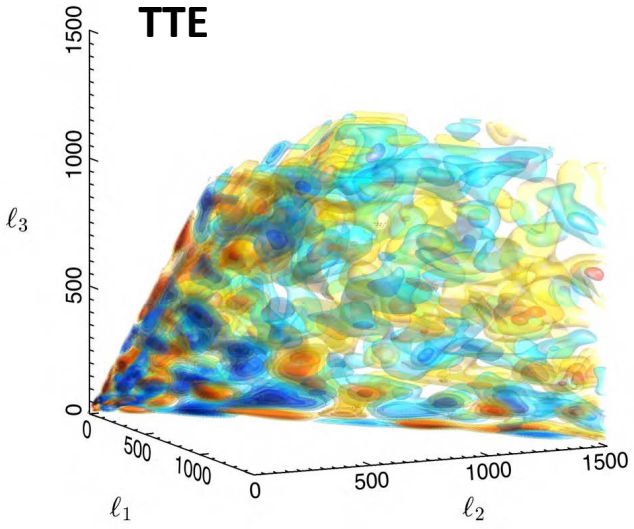

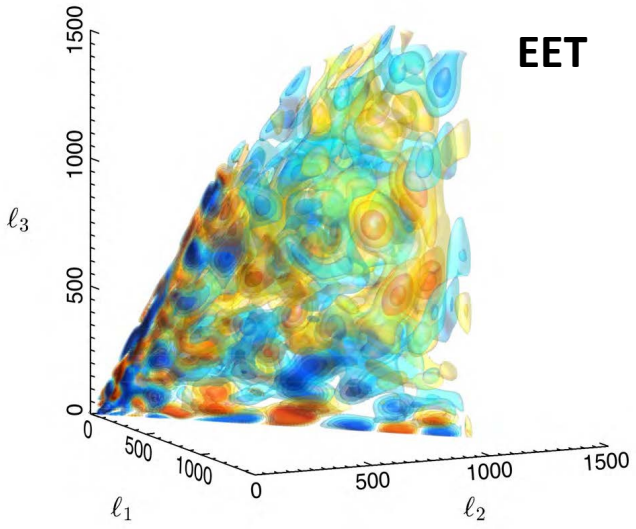

(S/N weighted)

f_{NL} from *Planck* 2018 bispectrum (KSW)

Shape and method	f_{NL}(KSW) Independent	f_{NL}(KSW) ISW-lensing subtracted	2015
SMICA (T)			
Local	5.9 ± 5.5	-1.6 ± 5.5	1.8 ± 5.6
Equilateral	13 ± 66	14 ± 66	−9.2 ± 69
Orthogonal	-37 ± 36	-15 ± 36	−20 ± 33
SMICA (T+E)			
Local	4.1 ± 5.1	-0.83 ± 5.1	0.71 ± 5.1
Equilateral	-17 ± 47	-18 ± 47	−9.5 ± 44
Orthogonal	-46 ± 23	-37 ± 23	−25 ± 22

$l_{min}=4$

Preliminary

Evolution of CMB constraints on inflation parameters

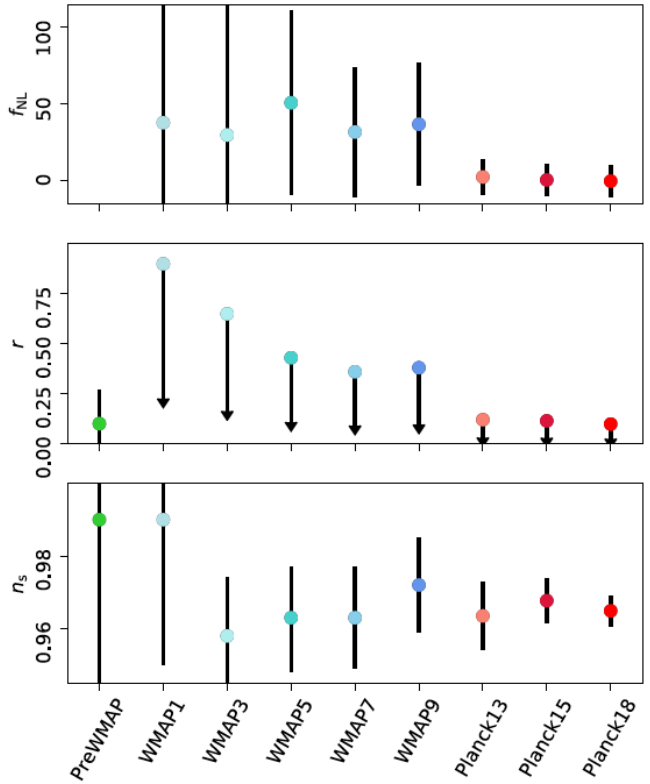

Planck collaboration 2018 (legacy paper)

Fig. 11. Evolution of CMB constraints on parameters describing "early Universe physics," specifically the amount of primordial, local non-Gaussianity (f_{NL}), the tensor-to-scalar ratio (r), and the slope of the primordial power spectrum (n_s).

PNG and precision cosmology

- PNG is currently the highest precision test of Standard Inflation models.

- With Planck:
  - PNG constrained at better than ~ 0.01%
  - Flatness constrained at ~ 0.1%
  - Isocurvature mode constrained at ~ 1%.

ISW-lensing bispectrum from *Planck*

The coupling between weak lensing and Integrated Sachs-Wolfe (ISW) effects is the leading contamination to local NG. We have detected the ISW-lensing bispectrum with a significance of ~ 3σ. This determination is also robust to SZ removal (2019).

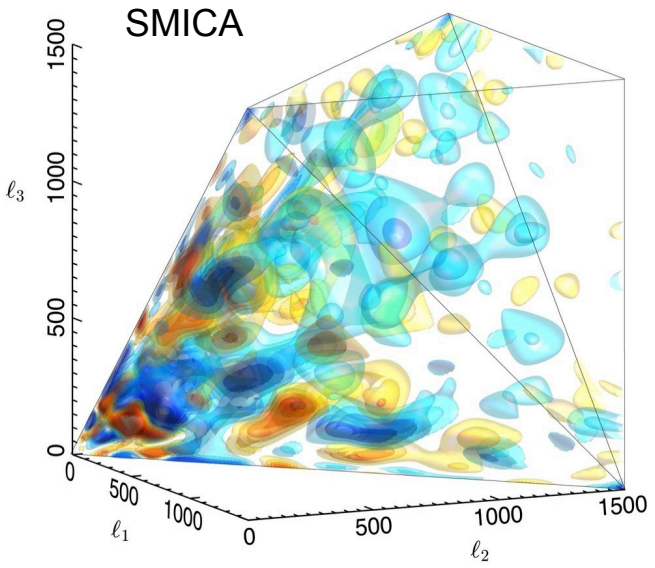

SMICA (T+E)	SMICA-noSZ (T+E)
$f_{NL}^{ISW-lensing} = 0.81 \pm 0.27$	$f_{NL}^{ISW-lensing} = 0.90 \pm 0.28$

Preliminary

Skew-C_l detection of ISW-lensing signal

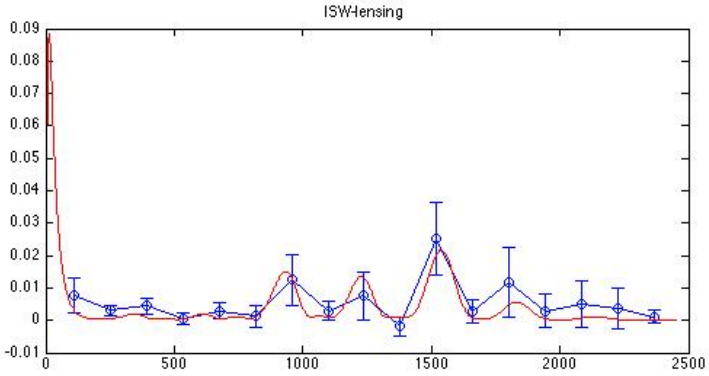

Planck 2013

Planck constraints on primordial trispectrum amplitudes

- In the 2018 release we obtain also constraints on 3 fundamental shapes of the trispectrum (transform of 4-pt function)

Trispectrum	Value
g_{nl}^{loc}	$(-5.3 \pm 9.3)\times 10^4$
$g_{nl}^{\dot{\pi}^4}$	$(-2.1 \pm 2.0)\times 10^6$
$g_{nl}^{(\partial\pi)^4}$	$(-6.0 \pm 5.0)\times 10^6$

Preliminary

Standard inflation still alive … and kicking!

Standard inflation

- single scalar field (*single clock*)
- canonical kinetic term
- slow-roll dynamics
- Bunch-Davies initial vacuum state
- Einstein gravity

predicts tiny (up to $O(10^{-2})$, or even less??) primordial NG signal

→ No presently detectable PNG

Beyond “standard” shapes

We constrain f_{NL} for a large number of primordial models beyond the standard local, equilateral, orthogonal shapes, including

- ✓ Equilateral family (DBI, EFT, ghost)
- ✓ Flattened shapes (non-Bunch Davies)
- ✓ Feature models (oscillatory bispectra, scale-dependent)
- ✓ Direction dependence
- ✓ Quasi-single-field
- ✓ Parity-odd models

- No evidence for PNG found → constraints on parameters from the models above

CORE: CMB bispectrum forecasts

	LiteCORE 80	LiteCORE 120	**CORE M5**	COrE+	Planck 2015	LiteBIRD	ideal 3000
T local	4.5	3.7	**3.6**	3.4	(5.7)	9.4	2.7
T equilat	65	59	**58**	56	(70)	92	46
T orthog	31	27	**26**	25	(33)	58	20
T lens-isw	0.15	0.11	**0.10**	0.09	(0.28)	0.44	0.07
E local	5.4	4.5	**4.2**	3.9	(32)	11	2.4
E equilat	51	46	**45**	43	(141)	76	31
E orthog	24	21	**20**	19	(72)	42	13
E lens-isw	0.37	0.29	**0.27**	0.24		1.1	0.14
T+E local	2.7	2.2	**2.1**	1.9	(5.0)	5.6	1.4
T+E equilat	25	22	**21**	20	(43)	40	15
T+E orthog	12	10.0	**9.6**	9.1	(21)	23	6.7
T+E lens-isw	0.062	0.048	**0.045**	0.041		0.18	0.027

from: Finelli et al. 2018

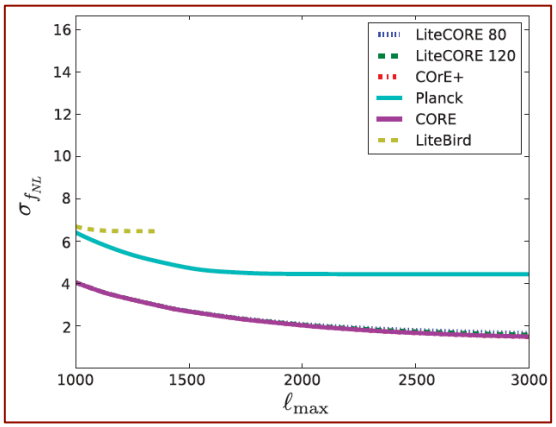

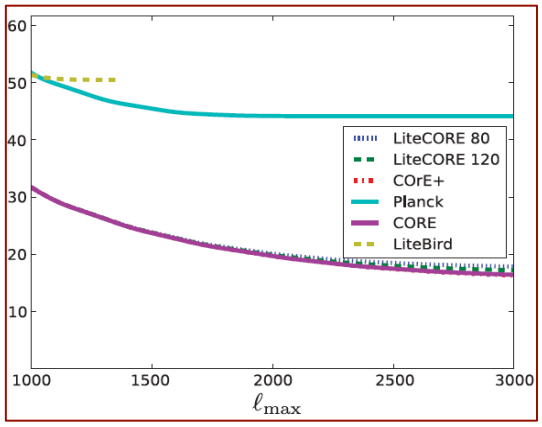

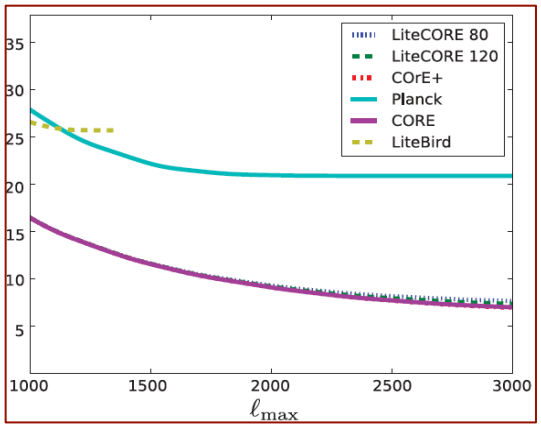

Primordial Non-Gaussianity (PNG) & the Large-Scale Structure (LSS) of the Universe

(= primordial NG + NG from gravitational instability)

PNG vs. Large-Scale Structure (LSS)

PNG in LSS (to make contact with the CMB definition) can be defined through a potential Φ defined starting from the DM density fluctuation δ through Poisson's equation (use comoving gauge for density fluctuation, Bardeen 1980)

$$\delta = -\left(\frac{3}{2}\Omega_m H^2\right)^{-1} \nabla^2 \Phi$$

Assuming the same model

$$\Phi = \phi_L + f_{NL}(\phi_L^2 - \langle\phi_L^2\rangle) + g_{NL}(\phi_L^3 - \langle\phi_L^2\rangle\phi_L) + \ldots$$

Φ on sub-horizon scales reduces to minus the large-scale gravitational potential, ϕ_L is the linear Gaussian contribution and f_{NL} and g_{NL} are dimensionless non-linearity parameters (or more generally non-linearity functions).

CMB and LSS conventions may differ by a factor 1.3 for f_{NL}, $(1.3)^2$ for g_{NL}

N-body simulations with NG initial data

$$\Phi = \Phi_L + f_{NL}(\Phi_L^2 - \langle \Phi_L^2 \rangle)$$

$$\nabla^2(\Phi * T)g(z) = -4\pi G a^2 \delta\rho_{DM}$$

growth suppression factor

matter transfer function

Grossi, Moscardini, Dolag, Branchini, Matarrese & Moscardini (2007)

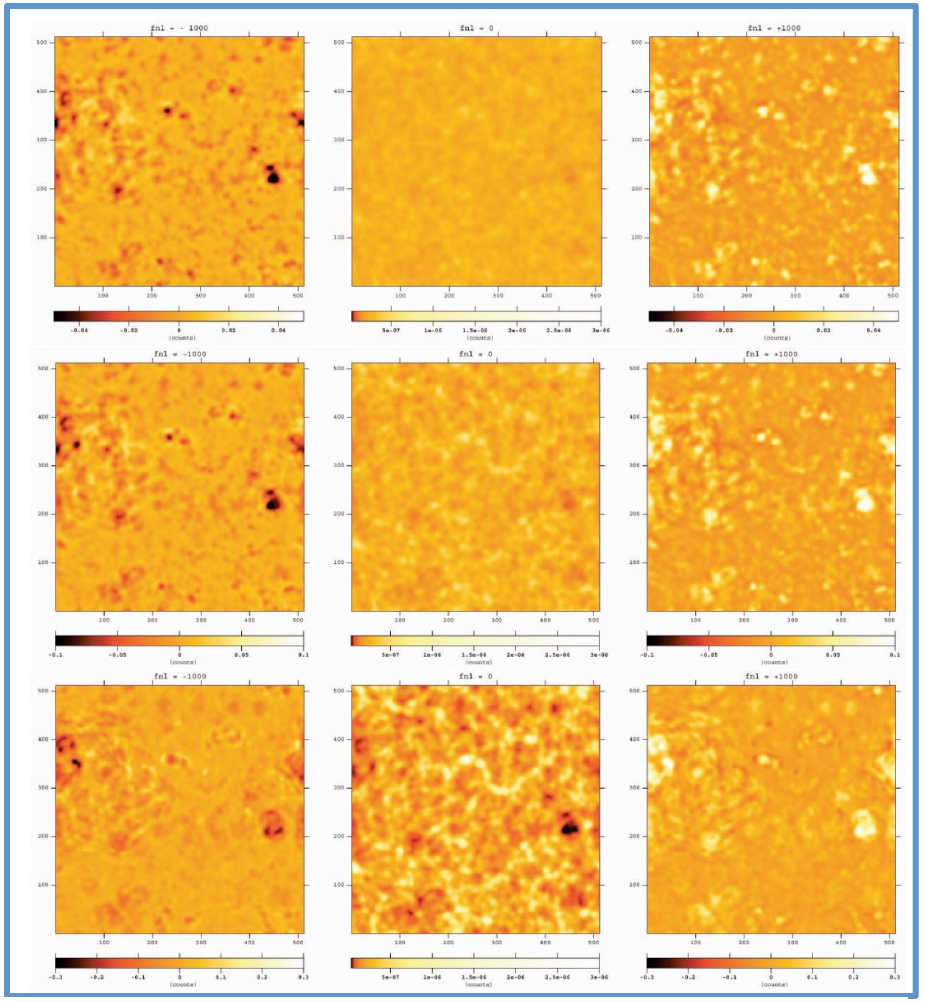

Figure 1. Slice maps of simulated mass density fields at $z = 5.15$ (*top*), $z = 2.13$ (*middle*) and $z = 0$ (*bottom*). The number of pixels at a side length is 512 ($500h^{-1}$Mpc) and that of the thickness is 32 ($31.25h^{-1}$Mpc). The panels in the middle row show the log of the projected density smoothed with a Gaussian filter of 10 pixels width, corresponding to $9.8h^{-1}$Mpc. The left and right panels are the relative residuals for the $f_{NL}=\pm 1000$ runs (equation [17]). Each panel has the corresponding color bar and the range considered are different from panel to panel.

Searching for PNG with rare events

- Besides using standard statistical estimators, like (mass) bispectrum, trispectrum, three and four-point function, skewness, etc. …, one can look at the tails of the distribution, i.e. at rare events.

- Rare events have the advantage that they often maximize deviations from what is predicted by a Gaussian distribution, but have the obvious disadvantage of being rare! But remember that, according to Press-Schechter-like schemes, all collapsed DM halos correspond to (rare) high peaks of the underlying density field (note: density, not gravitational potential maxima).

- Analogous to hot and cold spots in CMB maps (Matarrese & Vittorio (2019, in preparation), extending previous work on Gaussian fields (Vittorio & Juszkiewicz 1987).

- Matarrese, Verde & Jimenez (2000) and Verde, Jimenez, Kamionkowski & Matarrese (2001) showed that clusters at high redshift ($z>1$) can probe NG down to $f_{NL} \sim 10^{2.}$ Many more analyses and predictions afterwards. Excellent agreement of analytical formulae with N-body simulations found by Grossi et al. 2009; Desjacques et al. 2009; Pillepich et al. 2010; … and many others.

- Halo (galaxy) clustering 2-point and higher-order correlation functions represent further and more powerful implementations of this general idea (Dalal et al. 2007; Matarrese & Verde 2008; Giannantonio & Porciani 2010; Baldauf et al. 2011).

Bias: halos (hence galaxies) do not trace the underlying dark matter distribution

- Following the original proposal by Kaiser (1984), introuced for galaxy clusters and later for galaxies, we are used to parametrize our ignorance about the way in which DM halos clusters in space w.r.t. the underlying DM, via some "bias" parameters, e.g., for Eulerian bias

$$\delta_{halo}(x) = b_1 \delta_{matter}(x) + b_2 \delta^2_{matter}(x) + \ldots$$

or via some non-linear and non-local expression (e.g. as a function of the Lagrangian position of the proto-halo center of mass.

- The resulting non-linear and non-local terms affect the statistical distribution of the halos introducing further NG effects.
- Bias parameters can be generally dealt with either as purely phenomenological ones (i..e. to be fitted to observations) or predicted by a theory (e.g. Press-Schecter + Lagrangian PT).

Dark matter halo clustering as a powerful constraint on PNG

$$\delta_{halo} = b\, \delta_{matter}$$

Dalal, Dore', Huterer & Shirokov 2007

Dalal et al. (2007) have shown that halo bias is sensitive to primordial non-Gaussianity through a scale-dependent correction term (in Fourier space)

$$\Delta b(k)/b \;\alpha\; 2\, f_{NL} \delta_c / k^2$$

This opens interesting prospects for constraining or measuring NG in LSS but demands for an accurate evaluation of the effects of (general) NG on halo biasing.

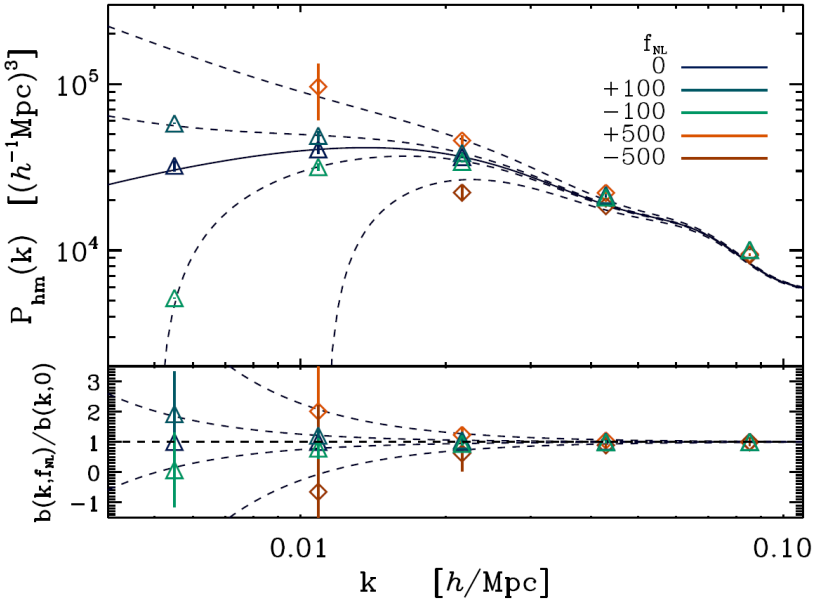

Clustering of peaks (DM halos) of NG density field

Start from results obtained in the 80's by Grinstein & Wise 1986 and Matarrese, Lucchin & Bonometto 1986 (see also Lucchin, Matarrese & Viittorio 1988), giving the general expression for the peak 2-point function as a function of N-point connected correlation functions of the background linear (i.e. Lagrangian) mass-density field

$$\xi_{h,M}\left(|\mathbf{x}_1 - \mathbf{x}_2|\right) = -1 +$$

$$\exp\left\{\sum_{N=2}^{\infty}\sum_{j=1}^{N-1}\frac{\nu^N\sigma_R^{-N}}{j!(N-1)!}\xi^{(N)}\begin{bmatrix}\mathbf{x}_1,\ldots,\mathbf{x}_1, & \mathbf{x}_2,\ldots\ldots,\mathbf{x}_2\\ j\,times & (N-j)\,times\end{bmatrix}\right\}$$

(requires use of path-integral, cluster expansion, multinomial theorem and asymptotic expansion). The analysis of NG models was motivated by a paper by Vittorio, Juszkiewicz and Davis (1986) on bulk flows.

THE ASTROPHYSICAL JOURNAL, 310:L21–L26, 1986 November 1

A PATH-INTEGRAL APPROACH TO LARGE-SCALE MATTER DISTRIBUTION ORIGINATED BY NON-GAUSSIAN FLUCTUATIONS

SABINO MATARRESE
International School for Advanced Studies, Trieste, Italy
FRANCESCO LUCCHIN
Dipartimento di Fisica G. Galilei, Padova, Italy
AND
SILVIO A. BONOMETTO
International School for Advanced Studies, Trieste, Italy; Dipartimento di Fisica G. Galilei, Padova, Italy; and INFN, Sezione di Padova
Received 1986 July 7; accepted 1986 August 1

ABSTRACT

The possibility that, in the framework of a biased theory of galaxy clustering, the underlying matter distribution be non-Gaussian itself, because of the very mechanisms generating its present status, is explored. We show that a number of contradictory results, seemingly present in large-scale data, in principle can recover full coherence, once the requirement that the underlying matter distribution be Gaussian is dropped. For example, in the present framework the requirement that the two-point correlation functions vanish at the same scale (for different kinds of objects) is overcome. A general formula, showing the effects of a non-Gaussian background on the expression of three-point correlations in terms of two-point correlations, is given.

Subject heading: galaxies: clustering

THE ASTROPHYSICAL JOURNAL, 310:19–22, 1986 November 1

NON-GAUSSIAN FLUCTUATIONS AND THE CORRELATIONS OF GALAXIES OR RICH CLUSTERS OF GALAXIES[1]

BENJAMIN GRINSTEIN[2] AND MARK B. WISE[3]
California Institute of Technology
Received 1986 March 6; accepted 1986 April 18

ABSTRACT

Natural primordial mass density fluctuations are those for which the probability distribution, for mass density fluctuations averaged over the horizon volume, is independent of time. This criterion determines that the two-point correlation of mass density fluctuations has a Zeldovich power spectrum (i.e., a power spectrum proportional to k at small wavenumbers) but allows for many types of reduced (connected) higher correlations. Assuming galaxies or rich clusters of galaxies arise wherever suitably averaged natural mass density fluctuations are unusually large, we show that the two-point correlation of galaxies or rich clusters of galaxies can have significantly more power at small wavenumbers (e.g., a power spectrum proportional to $1/k$ at small wavenumbers) than the Zeldovich spectrum. This behavior is caused by the non-Gaussian part of the probability distribution for the primordial mass density fluctuations.

Subject headings: cosmology — galaxies: clustering

Halo bias in NG models

- Matarrese & Verde 2008 applied this relation to the case of NG of the gravitational potential, obtaining the power-spectrum of dark matter halos modeled as high "peaks" (up-crossing regions) of height $\nu=\delta_c/\sigma_R$ of the underlying mass density field (Kaiser's model). Here $\delta_c(z)$ is the critical overdensity for collapse (at redshift a) and σ_R is the *rms* mass fluctuation on scale R ($M \sim R^3$).

- Account for motion of peaks (going from Lagrangian to Eulerian space), which implies (Catelan et al. 1998)

$$1+\delta_h(\mathbf{x}_{Eulerian}) = (1+\delta_h(\mathbf{x}_{Lagrangian}))(1+\delta_R(\mathbf{x}_{Eulerian}))$$

and (to linear order) $b=1+b_L$ (Mo & White 1996) to get the scale-dependent halo bias in the presence of NG initial conditions. *Corrections may arise from second-order bias and GR terms.*

- Alternative approaches (e.g. based on 1-loop calculations) by Taruya et al. 2008; Matsubara 2009; Jeong & Komatsu 2009. Giannantonio & Porciani 2010 improve fit to N-body simulations by assuming dependence on gravitational potential) → extension to bispectrum by Baldauf et al. 2011.

Halo bias in NG models

Matarrese & Verde 2008

$$b_{\rm h}^{f_{\rm NL}} = 1 + \frac{\Delta_c(z)}{\sigma_R^2 D^2(z)}\left[1 + 2 f_{\rm NL}\frac{\Delta_c(z)}{D(z)}\frac{\mathcal{F}_R(k)}{\mathcal{M}_R(k)}\right]$$

form factor:

$$\mathcal{F}_R(k) = \frac{1}{8\pi^2\sigma_R^2}\int dk_1 k_1^2 \mathcal{M}_R(k_1) P_\phi(k_1) \times \int_{-1}^{1} d\mu \mathcal{M}_R\left(\sqrt{\alpha}\right)\left[\frac{P_\phi\left(\sqrt{\alpha}\right)}{P_\phi(k)} + 2\right]$$

$$\alpha = k_1^2 + k^2 + 2k_1 k\mu$$

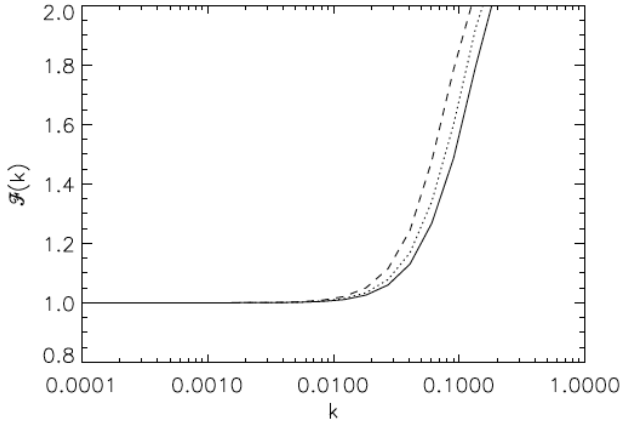

FIG. 1.— The function $\mathcal{F}_R(k)$ for three different masses: 1×10^{14} $M_\odot$ (solid), 2×10^{14} $M_\odot$ (dotted), 1×10^{15} $M_\odot$ (dashed).

factor connecting the smoothed linear overdensity with the primordial potential:

power-spectrum of a Gaussian gravitational potential

$$\mathcal{M}_R(k) = \frac{2}{3}\frac{T(k)k^2}{H_0^2\Omega_{m,0}}W_R(k)$$

transfer function:

window function defining the radius R of a proto-halo of mass M(R):

PNG with LSS: Bispectrum

Sample	Power Spectrum		Bispectrum	
	$\sigma_{f_{\rm NL}}$ bias float	$\sigma_{f_{\rm NL}}$ bias fixed	$\sigma_{f_{\rm NL}}$ bias float	$\sigma_{f_{\rm NL}}$ bias fixed
BOSS	21.30	13.28	$1.04^{(0.65)}_{(2.47)}$	$0.57^{(0.35)}_{(1.48)}$
eBOSS	14.21	11.12	$1.18^{(0.82)}_{(2.02)}$	$0.70^{(0.48)}_{(1.29)}$
Euclid	6.00	4.71	$0.45^{(0.18)}_{(0.71)}$	$0.32^{(0.12)}_{(0.35)}$
DESI	5.43	4.37	$0.31^{(0.17)}_{(0.48)}$	$0.21^{(0.12)}_{(0.37)}$
BOSS + Euclid	5.64	4.44	$0.39^{(0.17)}_{(0.59)}$	$0.28^{(0.11)}_{(0.34)}$

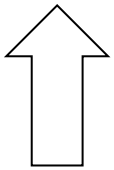

Tellarini et al. 2016

- Fisher matrix forecast. Tree-level bispectrum. Local NG initial conditions. In redshift space. Covariance between different triangles neglected (optimistic).
- The bispectrum could do better than the power-spectrum.
- $f_{NL} \sim 1$ achievable with forthcoming surveys?
- Many issues, e.g. full covariance, accurate bias model, GR effects, survey geometry, estimator implementation … Still, great potential: 3D vs 2D (CMB).

GR effects in the PS and bispectrum

- In full generality GR effects (including also redshift-space distortions, lensing, etc …) have to be taken into account both in the galaxy power-spectrum and bispectrum, as well as in the DM evolution.

- Bertacca, Raccanelli, Bartolo, Liguori, Matarrese & Verde (2017) have obtained for the first time the complete GR expression for the galaxy bispectrum (which is obviously VERY complex) to be soon compared with observations.

LSS initial conditions reconstruction to constrain/detect PNG

- PNG in LSS is contaminated by NG arising from non-linear gravitational evolution.

- Hence one can hope to improve PNG S/N by tracing LSS back in time and measure e.g. the bispectrum in reconstructed maps.

- Various reconstruction techniques have been proposed and tested, since the earliest proposal by Peebles (1989). For an application to PNG, see also Mohayaee, Mathis, Colombi & Silk 2006; based on MAK (Frisch, Matarrese, Mohayaee & Sobolevski 2002).

- Based upon recent results (Sarpa et al. 2018) aimed at reconstructing BAOs, Sarpa, Branchini, Carbone, Matarrese & Schimd are going to apply extended FAM algorithm (Nusser & Branchini 2000) to N-body simulations with non-Gaussian initial conditions.

BAO reconstruction: a swift numerical action method for massive spectroscopic surveys

arXiv:1809.10738 [astro-ph.CO]
submitted to MNRAS

E. Sarpa,[1,2]★ C. Schimd,[1] E. Branchini,[3,4,5] S. Matarrese.[2,6,7,8]

[1] *Aix Marseille Univ, CNRS, LAM, Laboratoire d'Astrophysique de Marseille, Marseille, France*
[2] *Dipartimento di Fisica e Astronomia "Galileo Galilei", Università degli studi di Padova, Via F. Marzolo, 8, I-35131 Padova, Italy*
[3] *Dipartimento di Matematica e Fisica, Università degli studi Roma Tre, Via della Vasca Navale, 84, 00146 Roma, Italy*
[4] *INFN - Sezione di Roma Tre, via della Vasca Navale 84, I-00146 Roma, Italy*
[5] *INAF - Osservatorio Astronomico di Roma, via Frascati 33, I-00040 Monte Porzio Catone (RM), Italy*
[6] *INFN, Sezione di Padova, via F. Marzolo 8, I-35131, Padova, Italy*
[7] *INAF-Osservatorio Astronomico di Padova, Vicolo dell'Osservatorio 5, I-35122 Padova, Italy*
[8] *Gran Sasso Science Institute, Viale F. Crispi 7, I-67100 L'Aquila, Italy*

Idea: Reconstruction of the *full* trajectories of biased tracers (haloes, galaxies, …) by minimisation of the action (Peebles 1989):

- orbits of i-th (point-like) object parametrised as $\mathbf{x}_i(D) = \mathbf{x}_{i,\mathrm{obs}} + \sum_{n=0}^{M} \mathbf{C}_{i,n} q_n(D)$, with $\mathbf{C}_{i,n}$ unknown: $\mathbf{C}_{i,n} = \operatorname{argmin} S$

$$\frac{S}{mH_0} = \sum_{i=0}^{N} \int_0^{D_{\mathrm{obs}}} dD f E D a^2 \frac{1}{2} \left(\frac{d\mathbf{x}_i}{dD}\right)^2 + \sum_{i=0}^{N} \int_0^1 dD \frac{3\Omega_{m0}}{8\pi f E D} \frac{1}{a} \left[\frac{1}{n_{\mathrm{obs}} a^3} \frac{1}{2} \sum_{j=0, j\neq i}^{N} \frac{1}{|\mathbf{x}_i - \mathbf{x}_j|} + \frac{2}{3} \pi \mathbf{x}_i^2 \right]$$

- mixed boundary conditions: observed positions + asymptotically vanishing initial velocities (i.e. initial homogeneity)
- FLRW universe (with generic, smooth dark-energy) + Newtonian approximation; equal mass particles; no merging

Target :

✷ Peebles ('90s):	Local group	~ 5 Mpc,	~ 10^3 particles
✷ Nusser & Branchini 2000 (FAM):	Local supercluster	~ 60 Mpc,	< 10^4 particles
✷ **Sarpa et al. 2018 (eFAM):**	**Large Scale Structure**	**~ 2 Gpc,**	**10^6 particles**

tested on dark-matter haloes from DEUS-FUR simulation

BAO reconstruction: a swift numerical action method for massive spectroscopic surveys

2-PCF: monopole in *redshift space*

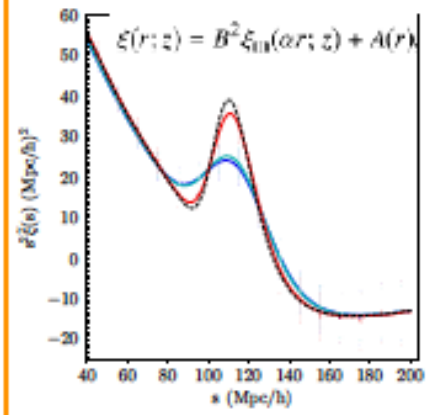

	Pre-rec	Post-rec
α BAO shift	1.007	0.997
σ_α	0.002	0.001
Σ_{nl} NL broadening	11.8 ± 0.3 h^{-1}Mpc	4.0 ± 0.5 h^{-1}Mpc

Pre reconstruction
Post-reconstruction z=0
Post-reconstruction, z = 33.6
Linear theory, *i.e. final goal*

2-PCF: quadrupole in redshift space

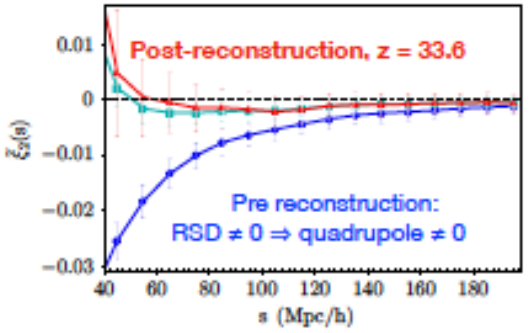

The new algorithm successfully reconstruct the BAO peak of linear theory, fully correcting for RSD on scale > 50 h^{-1}Mpc

2-PCF: anomalous mocks

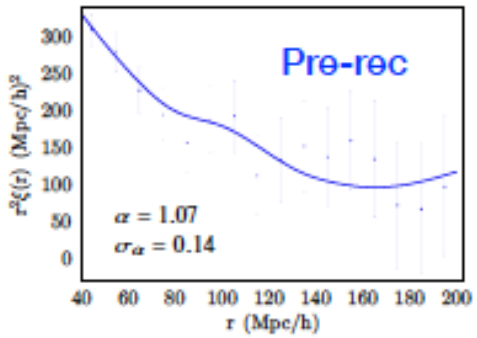

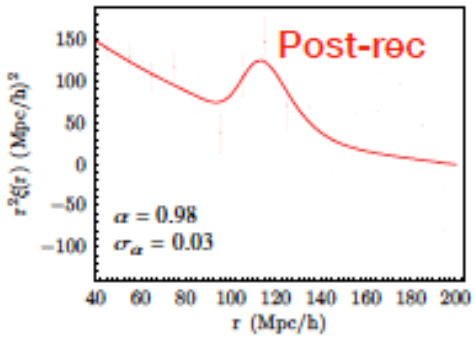

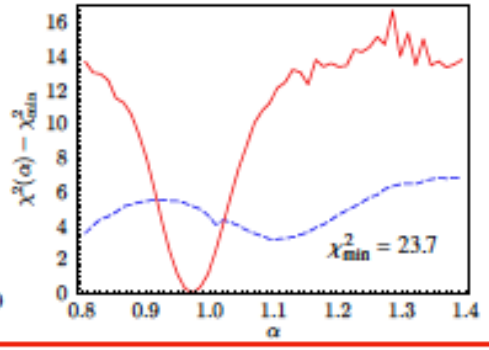

The new algorithm successfully recovers the BAO peak in statistically anomalous samples with unclear BAO peak (low S/N)

Anisotropic 2-PCF

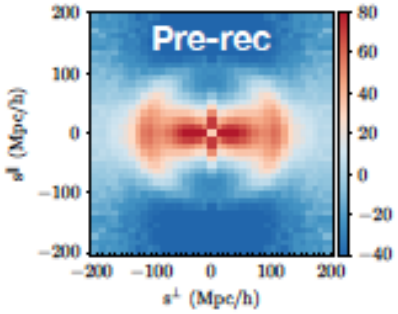

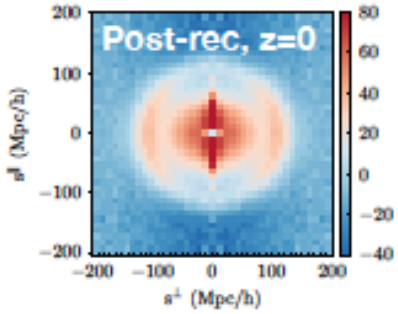

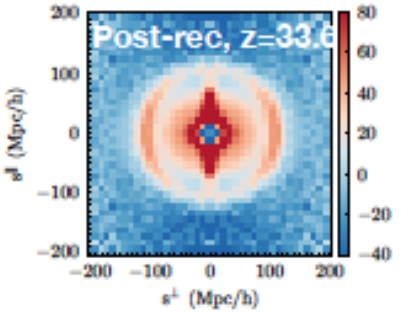

The new algorithm recovers the BAO ring at very-high S/N up to very large z (unlike standard method based on Zel'dovich approx, which *after smoothing* is limited to $z \sim 3$)

arXiv:1809.10738

Controversial issues on non-Gaussianity

Observability of GR non-linearities

- In the halo bias case the effect is unobservable. Indeed, as pointed out by Dai, Pajer & Schmidt 2015 and de Putter, Doré & Green 2015, a local physical redefinition of the mass, gauges way such a NG effect (*in the pure squeezed limit*), similarly to Maldacena's $f_{NL} = - 5/12(n_s-1)$ single-field NG contribution.

- This is true *provided the halo bias definition is strictly local*. Are there significant exceptions? Are all non-linear GR effects fully accounted for by "projection effects"?

- However, this dynamically generated GR non-linearity is physical and cannot be gauged away by any local mass-rescaling, provided it involves scales larger than the patch required to define halo bias, but smaller than the separation between halos (and the distance of the halo to the observer).

- Hence one would expect it to be in principle detectable in the matter bispectrum. Similarly, the observed galaxy bispectrum obtained via a full GR calculation must include all second-order GR non-linearities on such scales (*only as projection effects?*)

Concluding remarks

The Next Challenge

- Inflation provides a causal mechanism for the generation of cosmological perturbations
- CMB and LSS data fully support the detailed predictions of inflation
- The direct detection of:
  - primordial **gravitational waves**
  - primordial **non-Gaussianity**

  with the specific features predicted by inflation would provide strong independent support to the model.
- The next challenge is to measure $f_{NL} \sim 10^{-2}$